Agriculture **2015**, *5*, 538-560; doi:10.3390/agriculture5030538

OPEN ACCESS

agriculture

ISSN 2077-0472

www.mdpi.com/journal/agriculture

Article

Transferability of Models for Estimating Paddy Rice Biomass from Spatial Plant Height Data

Nora Tilly [1,*], Dirk Hoffmeister [1], Qiang Cao [2], Victoria Lenz-Wiedemann [1], Yuxin Miao [2] and Georg Bareth [1]

[1] ICASD-International Center for Agro-Informatics and Sustainable Development, Institute of Geography (GIS & Remote Sensing Group), University of Cologne, 50923 Cologne, Germany; E-Mails: dirk.hoffmeister@uni-koeln.de (D.H.); victoria.lenz@uni-koeln.de (V.L.-W.); g.bareth@uni-koeln.de (G.B.)

[2] ICASD-International Center for Agro-Informatics and Sustainable Development, Department of Plant Nutrition, China Agricultural University, 100193 Beijing, China; E-Mails: qiangcao@cau.edu.cn (Q.C.); ymiao@cau.edu.cn (Y.M.)

* Author to whom correspondence should be addressed; E-Mail: nora.tilly@uni-koeln.de; Tel.: +49-221-470-6265; Fax: +49-221-470-8838.

Academic Editor: Yanbo Huang

Received: 6 May 2015 / Accepted: 17 July 2015 / Published: 23 July 2015

Abstract: It is known that plant height is a suitable parameter for estimating crop biomass. The aim of this study was to confirm the validity of spatial plant height data, which is derived from terrestrial laser scanning (TLS), as a non-destructive estimator for biomass of paddy rice on the field scale. Beyond that, the spatial and temporal transferability of established biomass regression models were investigated to prove the robustness of the method and evaluate the suitability of linear and exponential functions. In each growing season of two years, three campaigns were carried out on a field experiment and on a farmer's conventionally managed field. Crop surface models (CSMs) were generated from the TLS-derived point clouds for calculating plant height with a very high spatial resolution of 1 cm. High coefficients of determination between CSM-derived and manually measured plant heights (R^2: 0.72 to 0.91) confirm the applicability of the approach. Yearly averaged differences between the measurements were ~7% and ~9%. Biomass regression models were established from the field experiment data sets, based on strong coefficients of determination between plant height and dry biomass (R^2: 0.66 to 0.86 and 0.65 to 0.84 for linear and exponential models, respectively). The spatial and temporal transferability of the models to

the farmer's conventionally managed fields is supported by strong coefficients of determination between estimated and measured values (R^2: 0.60 to 0.90 and 0.56 to 0.85 for linear and exponential models, respectively). Hence, the suitability of TLS-derived spatial plant height as a non-destructive estimator for biomass of paddy rice on the field scale was verified and the transferability demonstrated.

Keywords: terrestrial laser scanning; plant height; biomass; rice; precision agriculture; field level

1. Introduction

Solutions to ensure the world's food security are required due to the growing world population. Focusing on the supply with staple food, the cultivation of rice is essential. This is in particular for the Asian world important, where 2011 and 2012 about 90% of the estimated world rice production was cultivated, each year about 650 million tons [1]. Miao *et al*. [2] reviewed long-term experiments on sustainable field management and highlighted the required increase in cereal production to ensure food security in China. The authors emphasized the combination of traditional practices and modern sensor-based management approaches for addressing this challenge.

In this context, precision agriculture (PA) rises in importance, which focuses on spatial and temporal variabilities of natural conditions and an adequate dealing with resources [3]. PA-improved management methods support farmers in closing the gap between potential and current yield [4]. Based on analyses of long-term field experiments, Roelcke *et al*. [5] concluded that there is a great need for on-farm experiments. Therefore accurate crop monitoring based on remote and proximal sensing has become increasingly important within PA in recent years [6,7]. A widely used indicator for quantifying the actual status of plants is the nitrogen nutrition index (NNI) [8–10]. The index shows the ratio between measured and critical N content. The latter is determined by the crop-specific N dilution curve, showing the relation between N concentration and biomass. Consequently, the accurate and non-destructive determination of biomass is a precondition for calculating the NNI.

For rice, it has been shown that grain yield is positively correlated to biomass and nitrogen (N) translocation efficiency [11], but over-fertilization affects the nutrient balance in soil and groundwater. Consequently, the NNI should be used for optimizing rice production with PA-improved management methods. Therefore, non-invasive approaches for biomass estimation are of key importance as rice paddies should be entered with machinery as little as possible during the growing season. Satellite remote sensing images serve for estimating the actual biomass and yield of large paddy rice fields [12–16]. However, for monitoring within-field variability and more accurately estimating biomass, a higher spatial resolution is required. The potential of ground-based plant parameter measurements as input for biomass estimation models was recently demonstrated for rice, maize, cotton, and alfalfa [7]. However, therein, plant height was manually measured, which is prone to selection bias. A ground-based multi-sensor approach showed good results for predicting biomass of grassland [17]. For biomass estimation of paddy rice, *in-situ* approaches with hand-held sensors for measuring canopy reflectance provided good results [18–20]. Moreover, Confalonieri *et al.* [21] emphasized rice plant height as a key

factor for predicting yield potential and developed a model for estimating plant height increase, but accurate *in-situ* measurements of plant height on field level are rare. Although virtual geometric models of single rice plants in a high resolution exist [22,23], uncertainties remain about the transferability to the field, due to varying patterns of plant growth. Hence, accurate methods for determining plant height on field level are desirable.

Light detection and ranging (LIDAR) sensors have been increasingly used in vegetational studies since the 1980s [24]. *In-situ* studies confirmed the potential of ground-based LIDAR methods, also known as terrestrial laser scanning (TLS), for the assessment of plant parameters in agricultural applications. Previous studies focused on the acquisition of plant height [25], post-harvest growth [26], leaf area index [27], crop density [28,29], nitrogen status [30], or the detection of individual plants [31,32]. Moreover, the potential of TLS for estimating the biomass of small-grain cereals was emphasized [33–36]. Regarding the accuracy, Lumme *et al.* [33] found that estimated heights of cereal plants correlated with tape measurements. The high precision for mapping of maize plants was shown by Höfle [31]. Little research has been done so far on TLS *in-situ* measurements of paddy rice. Hosoi and Omasa [37] examined vertical plant area density as an estimator for biomass, achieved with a portable scanner in combination with a mirror. Besides, biomass estimations based on TLS-derived spatial plant height was evaluated for some of the fields considered in the presented study [38,39]. But as stated above, multi-annual on-farm experiments are necessary for achieving a comprehensive understanding of plant growth and developing objective sensor-based measuring methods and models for biomass estimations [2,5].

Based on the promising results of the single year analyses [38,39], this study focused on (I) the robustness of the method, (II) the spatial and temporal transferability of the models, and (III) a model improvement. For the latter, in addition to partially existing linear models, exponential models were established, as a better suitability of these models is denoted in other studies of biomass estimations over different growth stages [20,40,41]. In two consecutive growing seasons, rice fields were monitored during the pre-anthesis period. Based on the data sets of a field experiment, estimation models for biomass were established and then applied on a farmer's conventionally managed fields.

2. Data and Methods

2.1. Study Area

Heilongjiang Province in the northeast of China is an important region for agricultural production [42]. Almost 25% of the total area is covered by the Sanjiang Plain (~120,000 km^2). The regional climate with cold and dry winters and short but warm, humid summers is marked by the East Asian summer monsoon [43,44]. Three field sites around the city of Jiansanjiang (N 47°15′21″ E 132°37′43″) were considered in this study.

At the Keyansuo experimental station (Jiansanjiang, Heilongjiang Province, China) the same field experiment was monitored in 2011 and 2012 (Figure 1). For the experiment, nine N fertilizer treatments were repeated three times for the rice varieties *Kongyu 131* and *Longjing 21*. Hence, the field with a spatial extent of 60 m by 63 m consisted of 54 plots, each about 10 m by 7 m in size. A detailed description of the experimental set-up is given by Cao *et al*. [45]. Related to the amount of N input,

variations in plant height and biomass were expected. These differences were useful for the TLS monitoring approach to capture varying patterns of plant growth at one growing stage.

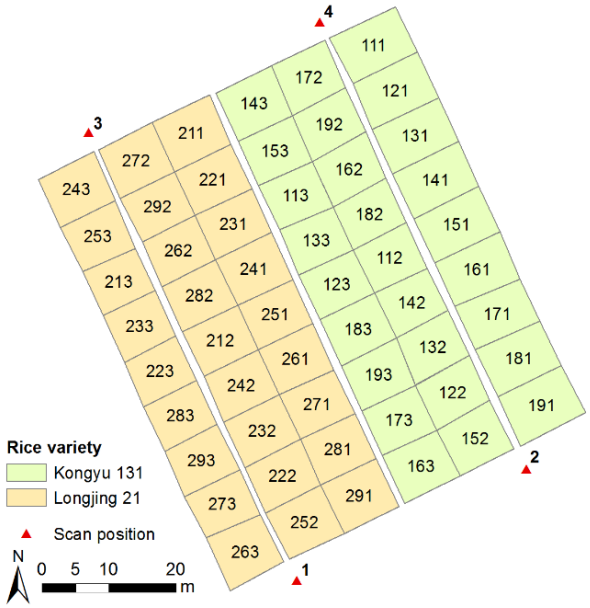

Figure 1. Design of the field experiment and scan positions. Three-digit number in the plot represents rice variety (1 = *Kongyu 131*; 2 = *Longjing 21*); treatment (1 to 9); and repetition (1 to 3). Modified from Tilly *et al*. [39].

In addition, one farmer's conventionally managed field was investigated each year (hereafter referred to as farmer's field). The aim was to provide independent validation data sets for checking the spatial and temporal transferability of the findings from the field experiment data. For the following, they are termed *village 69* (year 2011) and *village 36* (year 2012). In both years, it was not possible to find a field with one of the field experiment rice varieties, where destructive sampling was possible several times during the growing season. In *village 69* the variety *Kenjiandao 6* was cultivated, in *village 36* the variety *Longjing 31*. Moreover, in *village 36* management units with very heterogeneous development were chosen, including parts without any plants (Figure 2). On each field two management units were investigated. In *village 69* and *village 36* each unit was about 60 m by 40 m and 50 m by 70 m in size, respectively.

Figure 2. One management unit with very heterogeneous plant growth in *village 36*.

2.2. Field Measurements

On each site, three TLS campaigns were carried out in June and July of the respective year to capture the key vegetative stages of the rice plants. During this pre-anthesis period, differences in plant development occur mainly due to the increase of tillers and plant height. This period is important for fertilizer management decisions. In both years, the campaigns on the field experiment and the farmer's field were carried out on two consecutive days to reach a best possible comparison regarding the plant development. For quantifying the phenological stages of plants and steps in plant development the BBCH-scale was used [46,47]. The abbreviation BBCH is derived from the funding organizations: Biologische Bundesanstalt (German Federal Biological Research Centre for Agriculture and Forestry), Bundessortenamt (German Federal Office of Plant Varieties), and Chemical industry. The campaign dates and BBCH-values for all sites are given in Table 1.

Table 1. Dates of the terrestrial laser scanning (TLS) campaigns and corresponding phenological stages.

Date/	2011		2012	
BBCH-scale [a]	Field experiment	Village 69	Field experiment	Village 36
1. Campaign	21 June 2011/ 13	22 June 2011/ 13	1 July 2012/ 37	30 June 2012/ 37
2. Campaign	4 July 2011/ 13–15; 22–23	5 July 2011/ 13; 21	9 July 2012/ 42	8 July 2012/ 37; 39
3. Campaign	18 July 2011/ 19; 29; 32	19 July 2011/ 19; 29; 34	17 July 2012/ 50	16 July 2012/ 19; 29; 34

[a] Multiple values due to several samples.

Terrestrial laser scanners operating with the time-of-flight technique were used for all campaigns. The relative positions of survey points are calculated from the distances, as well as the horizontal and vertical angles between sensor and targets. For this, the time between transmitting and receiving a pulsed laser signal and its angles are measured. In 2011 and 2012, the Riegl VZ-1000 and Riegl LMS-Z420i, respectively, were provided by the company Five Star Electronic Technologies (Beijing, China) [48,49]. Both devices operate with a near-infrared laser beam and have a beam divergence of 0.3 mrad (VZ-1000) and 0.25 mrad (LMS-Z420i). The angular resolution was set to 0.04 deg. All scans were conducted from the dikes between the paddies to avoid entering them, resulting in an oblique perspective. More detailed descriptions are given in Tilly *et al*. [39].

The set-up for the campaigns on the field experiment was similar in both years. Each time, nine scan positions were established for covering all fields of the Keyansuo experimental station and minimizing shadowing effects. For this analysis, the scans from all positions were used, but four positions were of major importance, as they were located close to the investigated field experiment. Following, the largest number of points was acquired from these positions. Point clouds from other positions were used to avoid gaps in the final point cover due to information signs close to the field. As shown in Figure 1, two positions respectively were set up at the north and south edges. At each position the scanner was mounted on a tripod which raised the sensor up to 1.5 m above ground. Additionally, a small tractor-trailer system was

used for the positions at the south edge of the field for achieving a greater height of about 3 m. The narrow dikes along the other edges made it impossible to reach those positions with the tractor-trailer system.

Due to a limited access on the dikes between the management units of both farmer's fields, it was also impossible to use a trailer. Hence, the sensor height of the scanner on the tripod was about 1.5 m above ground. In *village 69* the scan positions were established close to the four corners of the management units (Figure 3). As the investigated units in *village 36* were located at the edge of the whole field, this set-up was slightly changed. Two positions in the north were established on a small hill close to the field for reaching a higher position and an additional position was placed at the center of the edge (scan position 5 in Figure 3). Further two positions were set up close to the south corners. In both fields, twelve thin, long bamboo sticks per management unit were stuck in the ground. These bamboo sticks can be easily detected in the TLS point clouds and located in the field to ensure the spatial linkage to other plant parameter measurements.

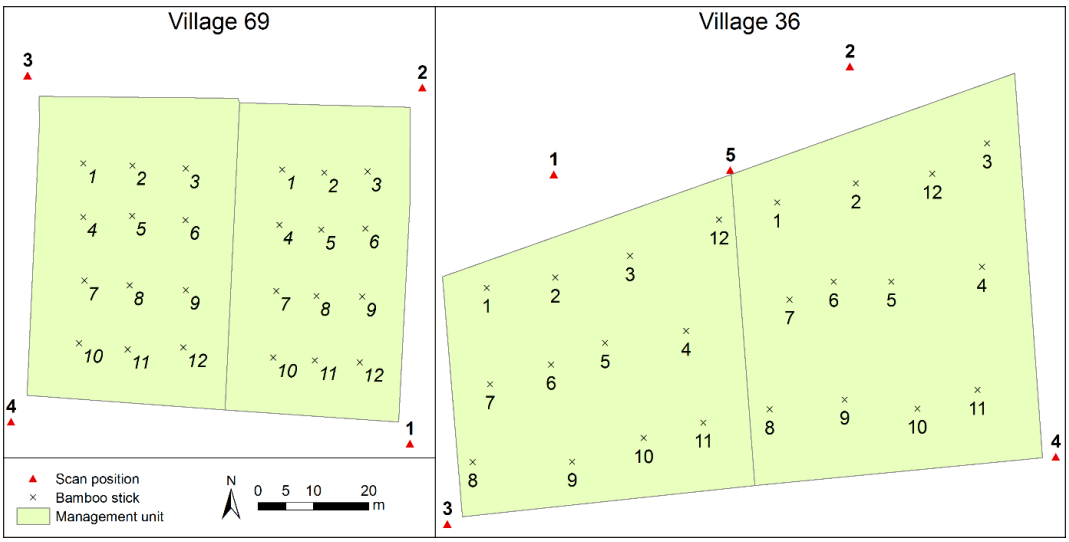

Figure 3. Scan positions and bamboo stick positions on the farmer's fields.

Furthermore, ranging poles with high-reflective cylinders [50] were built upon the dikes between the fields, homogeneously distributed around the field. These can be detected by the laser scanner and act as tie points for merging the scan data in post-processing. In the first campaigns, the position of each pole was marked in the fields. By re-establishing the ranging poles at exactly the same position for the following campaigns, all scans of one site can be merged. In the data sets from 2011, alignment errors occurred due to imprecise re-establishing of the ranging poles or where an exact marking of the positions was difficult, particularly on the farmer's fields. These errors could be rectified with software options but caused time-consuming post-processing. In 2012, additional tie points were used to avoid this. As shown in Figure 4 for *village 36*, five small, round reflectors were permanently attached to trees close to the fields and remained there during the observation period. A homogeneous distribution around the field was not possible, as no other stationary objects were available.

Figure 4. Small, round reflectors were permanently attached to trees in *village 36*.

At all sites, manual measurements of plant height and biomass were performed during the whole vegetation period. Corresponding to each TLS campaign on the field experiment, the heights of eight to ten and four hills per plot were measured in 2011 and 2012, respectively. Each hill consisted of four to six rice plants.

Regarding the measurement of biomass, differences between the sites and years must be pointed out. As part of the field experiment, destructive sampling was performed several times during the vegetation period. Samples were taken from both varieties, but only from the three repetitions of five treatments (n = 30). The dates of sampling differed from the TLS campaign dates in 2011, but due to the small plot size, it was not feasible to take additional samples. Thus, the biomass values were linearly interpolated. In 2012, the measurements could be carried out on the same day.

On the farmer's fields, four hills around each bamboo stick were destructively taken after the TLS measurements (each n = 24). For the following campaign, the bamboo sticks were moved in a defined direction to the center of four other hills. In each management unit of *village 36*, one bamboo stick was placed in the part without any plant and left at its position for all campaigns (no. 12 in Figure 3).

The cleaned above ground biomass was weighed after drying. All samples were oven dried at 105 °C for 30 min and dried to constant weight at 75 °C. The dry biomass per m^2 was calculated, considering the specific number of hills per m^2.

2.3. Post-Processing of the TLS Data

The post-processing of the scan data was similar for all sites. A detailed description is given for the data sets from 2011 in Tilly *et al*. [39]. Riegl's software RiSCAN Pro, also applied for the data acquisition, was used for the first steps of the data handling. The scans from all campaigns were imported into one RiSCAN Pro project file for each site. Following, a co-registration of all scan positions was carried out, based on the reflectors acting as tie points. As mentioned above, the data sets of 2011 showed alignment errors, due to non-optimal positioning or imprecise re-establishing of the ranging poles. The iterative closest point (ICP) algorithm [51], implemented in RiSCAN Pro as Multi Station Adjustment, was used to modify the position and orientation of each scan position in multiple iterations for getting the best fitting result. For the campaigns in 2012, additional small reflectors were permanently established. By first registering one scan position of each campaign based on these permanent tie points

and aligning all other positions to these, an accurate alignment was possible. After optimizing the alignment with the ICP algorithm the error, measured as standard deviation between the used point-pairs, was 0.06 m and 0.01 m on average for both sites of 2011 and 2012, respectively.

Following, the point clouds were merged to one data set per campaign and the area of interest (AOI) was manually extracted. Clearly identifiable noise in the point clouds far below and above the field, caused by reflections on water in the field or on small particles in the air, was previously removed. The crop surface was then determined from the point clouds with a filtering scheme for selecting maximum points. A common reference surface is required for the calculation of plant heights. Therefore, the AOI is usually scanned without any vegetation. As it was not possible to obtain such data on the rice fields, the lowest parts in the point clouds from the first campaigns were selected. At this stage, the rice plants were small enough for clearly identifying points at the bottom of the hills, as shown in Tilly *et al*. [39]. The point clouds of the field experiment data sets were subdivided plot-wise to attain a common spatial base. Each management unit of the farmer's fields was regarded as one data set. All data sets were exported as ASCII files, which contained the XYZ coordinates of each point for spatial and statistical analyses.

2.4. Calculation of Plant Height and Visualization as Maps of Plant Height

For the spatial analyses, crop surface models (CSMs) were constructed from the TLS-derived point clouds. CSMs were introduced by Hoffmeister *et al.* [50] for an objective and non-invasive deriving of spatial crop height and crop growth patterns. A CSM represents the crop surface at a specific date with a high spatial resolution. Therefore, the exported point clouds were interpolated to raster data sets with a consistent spatial resolution of 1 cm with the inverse distance weighting (IDW) algorithm in ArcGIS Desktop 10 (Esri, Redlands, CA, USA). IDW is suitable for preserving the accuracy of measurements with a high density, as it is a deterministic, exact interpolation and retains a measured value at its location [52]. Likewise, a digital terrain model (DTM) was generated from the manually selected ground points as common reference surface. Next, the DTM was subtracted from the CSM for calculating the plant heights. In the same way, plant growth between two dates can be spatially measured by calculating the difference between two CSMs. Herein, growth is defined as spatio-temporal difference in height. Finally, maps of plant height were created for visualizing the pixel-wise calculated values.

For the following analyses, one plant height value per campaign for comparable spatial units was necessary. Therefore, the CSM-derived plant heights were averaged plot-wise for the field experiment (n = 54). Previously, each plot was clipped with an inner buffer of 60 cm for preventing border effects. As the manual measurements were used for validating the laser scanning results, these plant height values were also averaged plot-wise (n = 54). Around each bamboo stick on the farmer's fields, a circular buffer with a radius of 1 m was generated to attain a common spatial base, for which the CSM-derived plant heights were averaged (each n = 24).

2.5. Estimation of Biomass

The field experiment analyses were taken to express the correlation between plant height and dry above ground biomass (hereafter referred to as biomass) in a biomass regression model (BRM). Since only the above ground plant height is determinable from the TLS data, statements about the

subsurface cannot be done. As mentioned above, other studies showed that exponential models performed better for biomass estimations over different growth stages. For establishing exponential models in addition to the linear ones, the biomass values were natural log-transformed. The models were used for estimating the biomass on the farmer's fields based on the TLS-derived spatial plant height data. Previously, linear and exponential biomass regression models (BRMs**)** were established, only regarding the field experiment for checking the general concept and evaluating differences between the results for 2011 and 2012 (hereinafter referred to as trial BRMs). Afterwards, the transferability of the model to the farmer's fields was evaluated. The workflow can be structured as following:

I. Examination of concept with trial BRMs: Each linear and exponential model was derived from the measurements of two field experiment repetitions from one year. The biomass of the remaining third repetition was estimated and validated against the destructive measurements.
II. Generation of BRM: Overall six models were established based on the measurements of all field experiment repetitions, separately for each year and as a combination of both years, each as linear and exponential model.
III. Application of the BRMs: Each model was used for estimating the biomass at all campaign dates on both farmer's fields based on the CSM-derived plant height of the buffer areas around the bamboo sticks.
IV. Validation of the BRMs: By comparing estimated and destructively measured biomass values the general validity, robustness, and suitability of the linear and exponential BRMs were evaluated.

The accuracy of each BRM was evaluated based on the coefficient of determination, index of agreement and root mean square error, calculated for each estimated value in comparison with the destructively measured biomass. The coefficient of determination (R^2) is widely used as measure of the dependence between two variables, but often unrelated to the size of the difference between them. For validating models, Willmott's index of agreement (d) shows to which degree a measured value can be estimated [53,54]. The index ranges between 0 and 1, from total disagreement to entire agreement. In addition, the root mean square error (RMSE) indicates how well the estimated values fit to the measured values [55].

3. Results

3.1. Maps of CSM-Derived Plant Height

The TLS-derived CSMs and the DTM were used to calculate plant height pixel-wise for all plots of the field experiment and each management unit of both farmer's fields. The resulting raster data sets have a high resolution of 1 cm. Maps of plant height were created for visualizing spatial and temporal patterns and variations. In Figure 5, maps of plant height are shown for two field experiment plots for all campaigns of both years. The respective first repetition of two fertilizer treatments for the rice variety *Kongyu 131* are selected as an example, whereby the plot numbers, 111 and 151, refer to the lower and higher amount of applied N fertilizer, respectively. In particular in the maps of plot 111, the linear structure of the rice plant rows is detectable in both years. In 2012, Plot 151 shows a discernible pattern with higher plant height values in the north corner, which is visible in all campaigns. Moreover, differences in plant height occur between the different fertilizer treatments. The mean plant heights are

higher for plots with a higher amount of applied N fertilizer, with a difference ranging from ~7 cm to ~13 cm and ~4 cm to ~16 cm for 2011 and 2012, respectively.

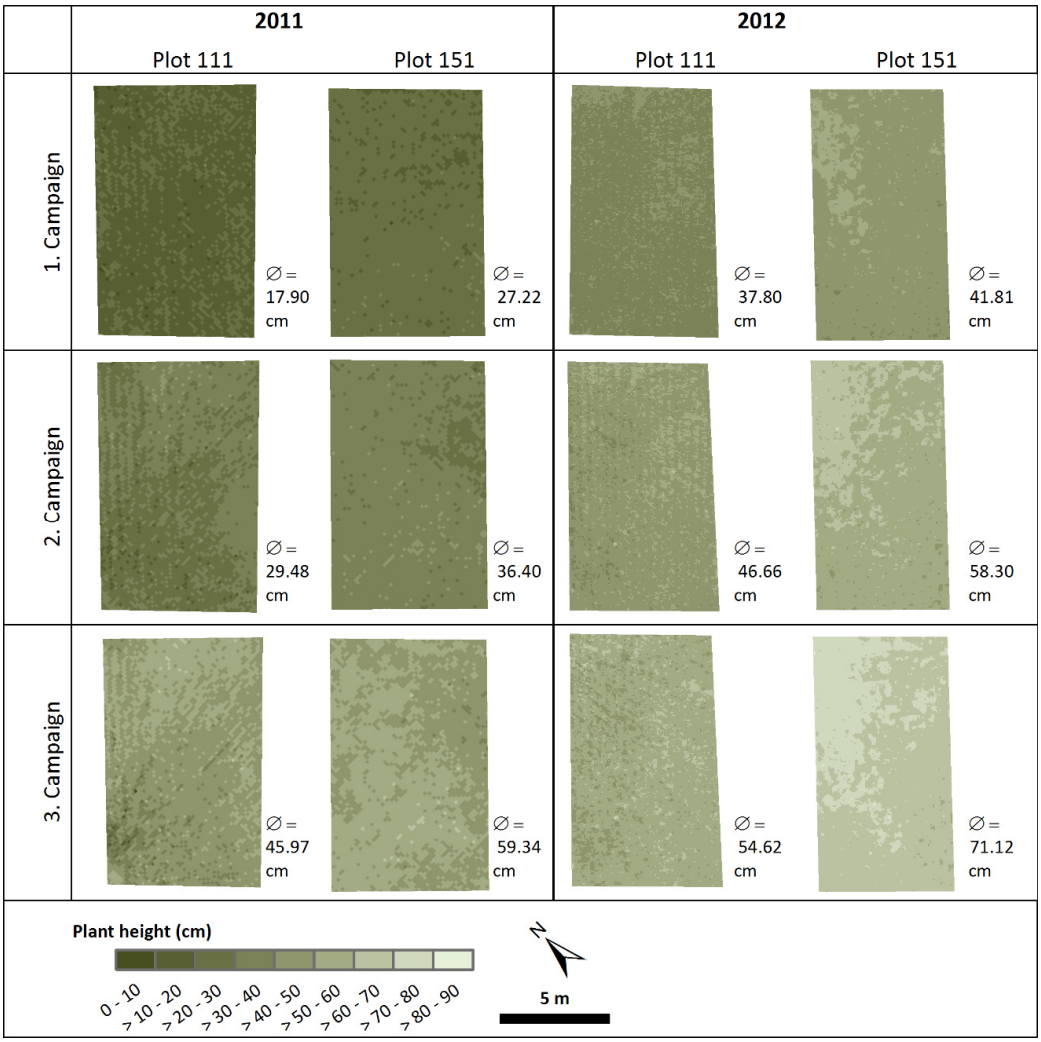

Figure 5. Crop surface model (CSM)-derived maps of plant height for two field experiment plots of both years, given with mean plant height per plot.

3.2. Analysis of Plant Height Data

Regarding the field experiment, averaged CSM-derived and manually measured plant heights were used for validating the accuracy of the scan data (Table 2). The mean heights are quite similar for both years, with an average difference of ~7% and ~9% for 2011 and 2012, respectively. The standard deviation within each campaign increases over time. All values and the resulting regression lines are shown in Figure 6. The coefficients of determination are high for 2011 and 2012 with $R^2 = 0.91$ and $R^2 = 0.72$, respectively.

Table 2. Mean crop surface model (CSM)-derived and manually measured plant heights of the field experiment (*n*, number of samples; $\bar{x}$, mean value; SD, standard deviation; min, minimum; max, maximum).

Date		Plant height from CSM (cm)				Measured plant height (cm)				Difference
	n	$\bar{x}$	SD	min	max	$\bar{x}$	SD	min	max	%
21 June 11	54	**24.84**	3.63	17.90	32.99	**24.37**	2.06	19.13	28.88	**1.89**
04 July 11	54	**34.62**	4.36	24.59	42.71	**37.94**	2.42	32.38	44.13	**9.59**
18 July 11	54	**55.38**	7.22	44.28	70.30	**63.56**	4.25	53.10	70.70	**14.77**
01 July 12	54	**44.72**	3.08	37.80	53.25	**40.85**	4.87	31.00	49.50	**8.64**
09 July 12	54	**57.09**	3.61	48.87	64.64	**46.84**	4.30	37.50	56.50	**17.95**

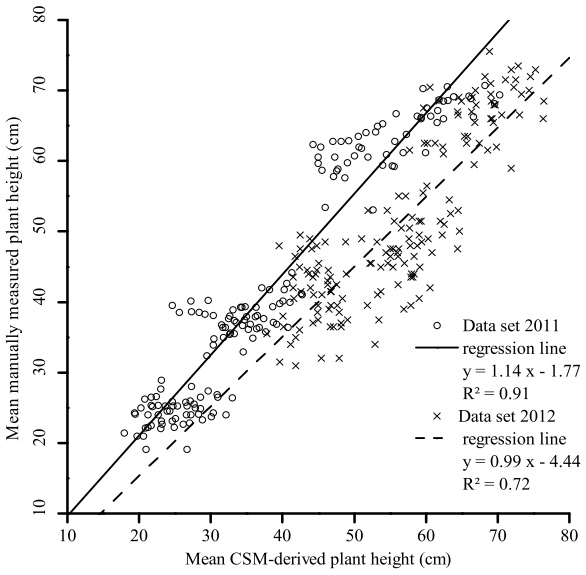

Figure 6. Regression of the mean CSM-derived and manually measured plant heights of the field experiment of both years (each *n* = 162).

3.3. Analysis of Estimated Biomass

Following the set-up of the field experiment, only five treatments were considered for the destructive biomass sampling (*n* = 30). Thus, the number of samples and averaged plant height values differ from the comparison shown in Table 2. On both farmer's fields, biomass was taken around all bamboo sticks (each *n* = 24). Mean value, standard deviation, minimum, and maximum were calculated for the plant height and dry biomass of all campaigns on each site (Table 3). The analysis of the mean plant heights can be summarized to: (I) the differences between the field experiment 2011 and *village 69* are less than ~5 cm, (II) the data sets from the field experiment 2012 and *village 36* show considerably larger differences with ~25 cm, (III) the difference between the data sets of the field experiment lies between ~10 cm and ~20 cm, (IV) comparing the farmer's fields, the difference increases over the growing season from ~2 cm to ~20 cm, and (V) the standard deviations within each campaign are almost similar and below ~5 cm, despite the results from *village 36* with values between ~6 cm and ~8 cm.

Regarding the biomass measurements, comparative statements have to be limited, due to the interpolated values for the field experiment 2011. Nevertheless, the results can be summed up as

following: (I) all mean values are considerable higher for 2012, (II) the difference between the values of the field experiment 2011 and *village 69* increases over time from less than 5% for the first campaign to ~40% and ~30% for the second and third campaign, respectively, (III) the difference between the values of the field experiment 2012 and *village 36* is constantly less than 5% during the whole observation period, and (IV) the standard deviation is much higher for all measurements in 2012, ranging from ~75 g/m^2 to ~145 g/m^2, in contrast to ~15 g/m^2 to ~80 g/m^2 for the measurements in 2011.

Table 3. Mean CSM-derived plant heights and destructively measured biomass values of all sites (*n*, number of samples; $\bar{x}$, mean value; SD, standard deviation; min, minimum; max, maximum).

Site/		Plant height from CSM (cm)				Biomass (g/m^2) [a]			
Date	*n*	$\bar{x}$	SD	min	max	$\bar{x}$	SD	min	max
Field experiment									
21.06.11	30	**24.93**	2.85	20.59	30.33	**59.51**	18.86	24.04	100.70
04.07.11	30	**33.80**	3.74	27.25	40.75	**131.72**	30.03	66.71	199.41
18.07.11	30	**56.69**	5.49	44.91	63.03	**422.27**	80.90	274.74	599.53
01.07.12	30	**43.81**	2.95	37.80	48.14	**231.42**	74.48	104.47	421.35
09.07.12	30	**56.08**	3.73	46.66	62.28	**449.92**	105.62	225.40	673.79
17.07.12	30	**66.63**	5.05	54.62	75.24	**636.10**	127.87	372.06	946.15
Village 69									
22.06.11	24	**20.80**	4.82	13.39	31.44	**57.58**	13.02	25.64	80.01
05.07.11	24	**34.09**	4.52	27.13	44.60	**217.43**	29.44	146.54	278.12
19.07.11	24	**59.49**	4.87	51.79	72.58	**589.71**	73.01	482.33	723.32
Village 36									
30.06.12	24	**18.13**	7.59	1.96	45.00	**251.67**	91.46	123.00	479.88
08.07.12	24	**30.23**	6.22	19.25	41.73	**469.93**	104.00	171.90	639.00
16.07.12	24	**40.36**	8.28	21.54	52.82	**717.61**	143.73	399.36	966.42

[a] values for the field experiment 2011 are linearly interpolated from other dates.

The regression equations from the field experiment data were used to establish linear and exponential BRMs. Previously, the general concept was examined with trial BRMs, each achieved from two field experiment repetitions of one year, validated against the third repetition. Table 4 shows the equations of the linear and exponential trial BRMs with the estimated and measured biomass values. In both years over- and underestimations occur, depending on the repetition combination and linear or exponential model. However, for the linear models the mean deviations of the estimated values from the actual measured values are small for 2011, less than 19% and very small for 2012, less than 1%. On the contrary, for 2011 the coefficients of determination (R^2) as well as the indices of agreement (d) between estimated and measured biomass values are higher and the root mean square error (RMSE) is lower. Similar R^2 and d values were achieved with the exponential models. Due to the log-transferred biomass values, the RMSE values cannot be directly compared. However, whereas the differences between estimated and measured values are much lower for 2011 (below 5%), they are slightly higher for 2012 (up to ~2.5%).

Table 4. Trial biomass regression models (BRMs) and validation of estimated against measured biomass (R^2, coefficient of determination; d, index of agreement; RMSE, root mean square error).

	Year/ Repetition	Trial BRMs [a]	Estimated Repetition	Mean biomass (g/m²) estimated	Mean biomass (g/m²) measured	Difference (%)	R^2	d	RMSE
Linear	**2011**								
	1 & 2	y = 11.06x − 211.23	3	249.79	210.61	−18.60	0.92	0.96	61.54
	1 & 3	y = 11.12x − 237.97	2	174.05	208.32	16.45	0.81	0.93	79.90
	2 & 3	y = 11.15x − 229.41	1	189.38	194.56	2.66	0.88	0.97	52.90
	2012								
	1 & 2	y = 14.33x − 379.96	3	427.12	426.06	−0.25	0.72	0.91	93.27
	1 & 3	y = 14.87x − 413.65	2	404.44	402.35	−0.52	0.55	0.85	125.13
	2 & 3	y = 14.36x − 379.12	1	413.28	417.20	0.94	0.71	0.91	92.77
Exponential [b]	**2011**								
	1 & 2	y = 0.06x + 2.76	3	4.99	5.22	4.58	0.88	0.95	0.38
	1 & 3	y = 0.06x + 2.64	2	5.01	4.83	−3.64	0.80	0.93	0.41
	2 & 3	y = 0.06x + 2.80	1	4.91	5.05	2.91	0.91	0.97	0.30
	2012								
	1 & 2	y = 0.04x + 3.79	3	5.95	5.96	0.22	0.68	0.89	0.28
	1 & 3	y = 0.04x + 3.82	2	5.88	6.02	2.44	0.58	0.82	0.36
	2 & 3	y = 0.04x + 3.67	1	5.94	5.88	−1.03	0.72	0.91	0.25

[a] x = plant height (cm); y = biomass (g/m²); [b] biomass values are natural log-transformed.

The final linear and exponential BRMs were established from the field experiment data sets for each year separately and for both years combined (Table 5). All values and the resulting regression lines are plotted in Figure 7 for the linear and exponential models, the corresponding equations are given in Table 5. Strong coefficients of determination for all data sets prove the dependency of biomass on plant height during the regarded pre-anthesis period. Comparable results were achieved for linear (2011: $R^2 = 0.86$; 2012: $R^2 = 0.66$; combination: $R^2 = 0.81$) and exponential models (2011: $R^2 = 0.84$; 2012: $R^2 = 0.65$; combination: $R^2 = 0.84$). Each model was used for estimating the biomass of the buffer areas around the bamboo sticks on both farmer's fields based on the CSM-derived plant height. The reliability of the estimated values was validated against the measured biomass values. In Table 5 the mean differences are given, averaged for each campaign and over all campaigns on each farmer's field. Further, the coefficient of determination (R^2), index of agreement (d), and root mean square error (RMSE) are given for each BRM. Generally, the estimations for *village 69* are better overall, verifiable through smaller percentage deviations, higher R^2 and d as well as lower RMSE values for linear and exponential models. The differences between linear and exponential models for each site are small with slightly better R^2 values for the linear BRMs. Within each site, the three models yielded almost similar results. Regarding the BRMs of the single years, the linear function showed slightly lower percentage deviations with the data set from 2011, whereas the exponential with the one from 2012. For the combined data set, the linear model functioned slightly better than both single year BRMs, whereas with the exponential models it performed weaker.

Table 5. Biomass regression models (BRMs), derived from field experiment and validation of estimated against measured biomass for the farmer's fields (R^2, coefficient of determination; d, index of agreement; RMSE, root mean square error).

	Site/	BRM [a]	Mean difference per campaign (g/m²)			Mean difference all campaigns		R^2	d	RMSE
	Data set		1.	2.	3.	(g/m²)	%			
Linear	**Village 69**									
	2011	y = 11.06x − 224.18	51.69	64.56	110.79	90.73	31.48	0.90	0.92	119.70
	2012	y = 14.51x − 390.58	146.33	113.35	115.10	125.59	43.57	0.90	0.91	146.90
	combination	y = 12.37x − 273.19	73.47	68.95	98.30	89.83	31.16	0.90	0.93	115.22
	Village 36									
	2011	y = 11.06x − 224.18	254.34	320.62	380.60	336.87	74.48	0.60	0.53	377.04
	2012	y = 14.51x − 390.58	281.90	382.73	425.57	375.82	83.09	0.60	0.51	429.33
	combination	y = 12.37x − 273.19	175.02	330.06	383.54	312.30	69.04	0.60	0.53	383.62
Exponential [b]	**Village 69**									
	2011	y = 0.06x + 2.74	0.04	0.59	0.32	0.23	4.35	0.85	0.95	0.46
	2012	y = 0.04x + 3.76	−0.58	0.25	0.24	−0.03	−0.65	0.85	0.92	0.45
	combination	y = 0.05x + 2.95	0.07	0.72	0.58	0.41	7.81	0.85	0.91	0.56
	Village 36									
	2011	y = 0.06x + 2.74	1.58	1.52	1.42	1.47	24.31	0.56	0.44	1.47
	2012	y = 0.04x + 3.76	0.65	1.12	1.13	0.97	15.97	0.56	0.51	1.06
	combination	y = 0.05x + 2.95	1.38	1.62	1.58	1.51	24.92	0.56	0.42	1.51

[a] x = plant height (cm); y = biomass (g/m²); [b] biomass values are natural log-transformed.

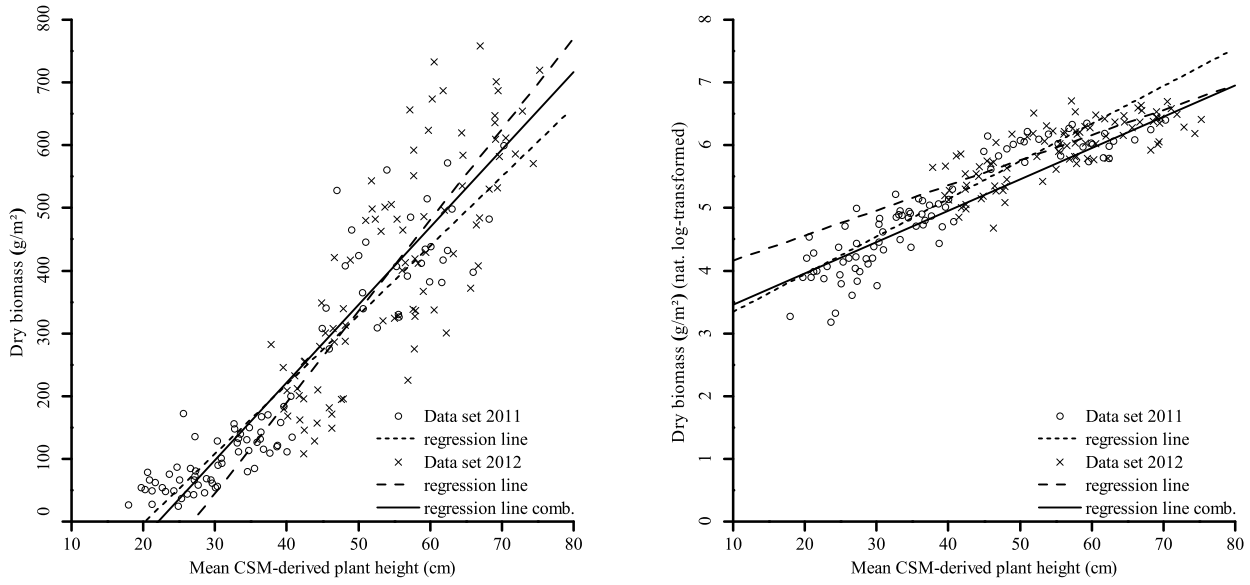

Figure 7. Linear (**left**) and exponential (**right**) regression between mean CSM-derived plant height and dry biomass for the field experiment of both years (each n = 90); regression equations are given in Table 5. Biomass values for the exponential regression are natural log-transformed.

4. Discussion

Overall, the acquisition with both laser scanners worked very well. The reliability of the devices was shown in earlier studies [38,39,50]. Due to the lightweight build-up and higher measurement rate the Riegl VZ-1000 is preferable to the Riegl LMS-Z420i, but was not available in 2012. As mentioned, alignment errors in the data sets from 2011 caused time-consuming post-processing. The positioning of additional reflectors was helpful for aligning the data sets from 2012 and led to better results, reflected by the lower error after the whole alignment process. A further source of error in TLS measurements is noise in the point cloud, caused by reflections on rain, insects, or other small particles in the air. Due to the small size of the measured crops and uneven surfaces, this issue has to be regarded in particular for applications in agriculture, as also reported from other studies [33,35]. The measuring speed of the used time-of-flight scanners reduced the noise already and filter options in RiSCAN Pro simplified its removal, but further developments are desirable. In this context, intensity values should be investigated for establishing filtering schemes. So far, they are used for separating laser returns on canopy from ground returns [56] or for detecting single plants [31,32].

Regarding the practical implementation, this approach indicates advantages towards similar studies. Good results were achieved for estimating biomass of rice plants based on the vertical plant area density, measured with a portable scanner in combination with a mirror [37]. However, for the application on larger-scale fields their set-up might be less practical. Through the non-invasive TLS acquisition from the edges of the field, undisturbed plant growth can be ensured and the scan positions with the tractor-trailer system profited from the greater height. As the linear structure of the rice plant rows is observable, a more precise acquisition of the crop surface can be assumed. Thus, lightweight scanners are desirable, which can easier be brought to a lifted position. Moreover, cost-effective systems like the Velodyne HDL-64E LiDAR sensor [57] and mobile laser scanning systems like the ibeo ALASCA XT [58] should be considered for realizing practical applications of the presented approach for farmers.

Further, the oblique perspective of the scanner must be taken into account, which is unavoidable from a ground-based system without entering the field. Studies indicate that the height of reflection points might be overestimated through the influence of the scanning angle [59]. As the measured signal is influenced by the scanning geometry and beam divergence [31,60], a radiometric calibration is supported for stationary TLS by other studies [26,61]. In this study, the merged and cleaned point clouds were filtered with a scheme for selecting maximum points. Hence, the crop surface was determined from an evenly distributed coverage of the field and overestimations should be precluded.

Manual measurements of plant height were conducted for validating the TLS data. However, therein differences between the measurement methods must be denoted. Whereas with less than ten hills per field experiment plot, only a small and mostly the highest part of the entire crop surface was considered for the manual measurements, the scanner captures the whole plot, including the lower parts. Hence, only plot-wise averaged values could be compared but the high R^2 values up to 0.91 between both measurements confirmed the accuracy of the TLS data. However, the approach of using the 90th percentile [36] instead of the maximum values for the CSM-based plant height calculation should be considered for achieving values which are more robust against low scanning resolutions. Generally, the precision of the TLS-derived CSMs is difficult to determine by the manual measurements due to these differences. The good performance of TLS measurements for agricultural applications is presumed from

other studies [31,33] and performance tests by the manufacturer validate the high accuracy and precision of the Riegl scanners [48,49]. Nevertheless, a main advantage is the objective assessment of plant height by CSMs, which avoids the selection bias of manual measurements. The non-invasive acquisition of the whole area in a high spatial resolution is one of the main benefits of the presented approach. In the context of PA, this is required for accurate crop monitoring [6].

Considering the upscaling of known plant information, the transferability of the virtually modelled geometry of single rice plants to field level might be evaluated with the high resolution CSMs [22,23]. Referring to the model of predicting yield potential for rice [21], the CSM-derived plant heights can be used as input data. Border effects cause problems in estimating rice yield, due to differences between internal and external rice plants in a plot [62]. In this study, an inner buffer was used to avoid border effects. For further studies, the high resolution of the TLS-derived CSMs might be useful for determining the differences between internal and external rows.

The pixel-wise calculated plant heights were visualized in maps of plant height for discovering spatial or temporal patterns and variations. As shown in Figure 5 the high resolution of 1 cm allowed an exact representation. In contrast, rice field mapping based on space-borne data has not been carried out with resolutions finer than 1 m so far [12,15,16]. However, new satellites like the WorldView-3 [63], providing a panchromatic resolution of ~0.3 m, should enable a more detailed acquisition. The high resolution is one of the major advantages of TLS data and enables the usability as *in-situ* validation for space-borne data. Although, the spatial extent of air- or space-borne methods cannot be reached with ground-based methods and the data acquisition effort is high, they are more flexible for the application in the field. Consequently, the presented approach may offer a tool for comparative analyses between TLS and airborne laser scanning (ALS). As shown by Bendig *et al*. [64] good results were achieved for the creation of CSMs from unmanned aerial vehicle (UAV)-based imaging for barley (R^2 up to 0.82 between CSM-derived and manually measured plant heights). Furthermore, promising results for the assessment of trees have already been achieved with UAV-based laser scanning systems [58,65]. However, the influence of the oblique and nadir scanning perspectives of ground- and air-borne measurements, respectively, have been less investigated so far. A comparative study on TLS and common plane-based ALS showed that the scanning angle and possible resolution influences the results [66]. Therefore, multiple sensors and acquisition levels should be combined for comprehensive analyses.

For confirming the general validity of spatial plant height data as a non-destructive estimator for biomass of paddy rice and proving the robustness as well as the spatial and temporal transferability of all established models, destructive biomass sampling was performed on all sites, revealing differences between the fields (Table 3). Basic differences were a lower human impact and larger size of the management units on the farmer's fields as well as the presence of different rice varieties and fertilizer treatments on all sites.

The three repetitions of each fertilizer treatment on the field experiment were useful to set up trial BRMs for proving the general concept (Table 4). High coefficients of determination and indices of agreement between the estimated and measured biomass values for each repetition of both years support linear and exponential models with comparable results. Nevertheless, further research is necessary for defining the differences between rice varieties and the influence of varying fertilizer treatments.

In addition to the final BRMs of each year, a model based on the combined data set of both years was established, each as a linear and an exponential model. The transferability of the BRMs from the small scale field experiment for estimating biomass on larger scale farmer's fields was shown (Table 5). Besides the transferability of existing models, a model improvement through the combined data set and through additional exponential models was investigated. As shown in Figure 7 for the data sets of the field experiment, the dependency of biomass on plant height can be described by linear and exponential regressions with similar high coefficients of determination. However, herein, only the pre-anthesis period was regarded. After anthesis, increasing biomass is mostly related to the development of grains while plant height remains almost constant. Thus, further studies are necessary for investigating the performance of linear and exponential BRMs for the estimation of rice biomass during the later stages.

The results of the linear and exponential models are almost similar for each site, with overall better values for *village 69*. As stated above the linear and exponential BRM yielded better results with the data sets from 2011 and 2012, respectively. A possible explanation might be the slightly different captured growth stages or the interpolated biomass values for 2011. Moreover, analyses are necessary, concerning the influence of different rice varieties, fertilizer treatments, or soil conditions. Additionally, the lower human impact on the farmer's fields might influence the plant development. For *village 36* the heterogeneous plant development in the management units has to be stated as a source for the differences between estimated and measured values. The varying performance of the combined model might be caused by these differences. Of most importance might be the fact that the relation between plant height and biomass in the two regarded periods seems to be best represented by different models. Overall, the results support the applicability of BRMs for biomass estimations based on TLS-derived spatial plant height data and substantiate the potential of ground-based plant parameter measurements as input for biomass estimation models [7,17].

5. Conclusions

The applicability and high suitability of terrestrial laser scanning for monitoring plant height of paddy rice based on multi-temporal CSMs were confirmed. An outstanding feature is the objective assessment of the whole field in a very high spatial resolution. Moreover, as the scans are non-invasively acquired from the field edges, entering the rice paddies is avoided. By investigating a repeated field experiment and two farmer’s conventionally managed fields in two years, varying patterns of plant development and growth were covered.

For PA, monitoring of plant parameters for adjusting site-specific fertilization is a major topic. Strong coefficients of determination between plant height and biomass show the applicability of spatial plant height data as a non-destructive estimator for biomass of rice plants. Based on the promising results of single year analyses [38,39], in this contribution, the annual transferability of the BRMs and the applicability on different fields were regarded. Moreover, a model improvement through exponential models was examined. During the regarded pre-anthesis period, the linear and exponential models performed equally well. Further studies are necessary regarding a presumed differing performance during the later stages. However, the spatial and temporal transferability of the BRMs to a larger scale is supported by estimations of biomass on farmer’s fields based on TLS-derived CSMs. High coefficients

of determination and indices of agreement between estimated and measured values demonstrate the coherence of the results and prove the robustness of the method. Regarding the accuracy of the estimation, best results were achieved with different models, depending on the used data. Overall, higher R^2 values were achieved with the linear models, whereas the exponential models yielded smaller percentage deviations.

To summarize, the novelty in this contribution is the comparative analysis of linear and exponential models based on objectively assessed plant height as a reliable estimator for the biomass of paddy rice over different growing seasons and different fields. Further long-term experiments and comprehensive monitoring approaches are required for investigating the performance of linear and exponential models for the pre-anthesis and for later growing stages.

In the future, combined approaches involving plant height and spectral measurements should be developed for accurately determining the actual biomass and N content of plants. Following, spatially resolved NNI calculations could be executed for improving N management strategies [67]. Thereby, over-fertilization could be reduced while keeping or enhancing the yield.

Acknowledgments

The accomplished field work was affiliated to the activities of the International Center for Agro-Informatics and Sustainable Development (ICASD). Founded in 2009 by the Department of Plant Nutrition of the China Agricultural University in Beijing and the Institute of Geography at the University of Cologne in Germany, ICASD is an open, international, and multidisciplinary cooperative research center (www.ICASD.org).

We would like to thank all colleagues and student assistants for their great effort during the field work (Juliane Bendig, Simon Bennertz, Jonas Brands, Erik Boger, Martin Gnyp, Anne Henneken, and Maximilian Willkomm). Further we extend our thanks to Five Star Electronic Technologies (Beijing, China), the Qixing Research and Development Centre and the Jiansanjiang Agricultural Research Station (both located in Heilongjiang Province, China) for good cooperation as well as RIEGL GmbH (Horn, Austria) for continuous support. This work was financially supported by the International Bureau of the German Federal Ministry of Education and Research (BMBF, project number 01DO12013) and the German Research Foundation (DFG, project number BA 2062/8-1).

Author Contributions

Nora Tilly with advice from Dirk Hoffmeister was responsible for the TLS measurements. The field experiment at the Keyansuo experimental station was carried out by Qiang Cao supervised by Yuxin Miao, who is scientific coordinator of the ICASD project, together with Victoria Lenz-Wiedemann. Nora Tilly carried out the post-processing and wrote this article, greatly supported by Dirk Hoffmeister and Victoria Lenz-Wiedemann. Georg Bareth directed the research and supervised the whole acquiring, analyzing, and writing process.

Conflicts of Interest

The authors declare no conflict of interest.

References

1. FAO FAOSTAT. Available online: http://faostat3.fao.org/faostat-gateway/go/to/home/E (accessed on 1 July 2014).
2. Miao, Y.; Stewart, B.A.; Zhang, F. Long-term experiments for sustainable nutrient management in China. A review. *Agron. Sustain. Dev.* **2011**, *31*, 397–414.
3. Oliver, M.; Bishop, T.; Marchant, B. An overview of precision agriculture. In *Precision Agriculture for Sustainability and Environmental Protection*; Oliver, M., Bishop, T., Marchant, B., Eds.; Routledge: London, UK, 2013.
4. Van Wart, J.; Kersebaum, K.C.; Peng, S.; Milner, M.; Cassman, K.G. Estimating crop yield potential at regional to national scales. *Field Crops Res.* **2013**, *143*, 34–43.
5. Roelcke, M.; Han, Y.; Schleef, K.H.; Zhu, J.-G.; Liu, G.; Cai, Z.-C.; Richter, J. Recent trends and recommendations for nitrogen fertilization in intensive agriculture in eastern China. *Pedosphere* **2004**, *14*, 449–460.
6. Mulla, D.J. Twenty five years of remote sensing in precision agriculture: Key advances and remaining knowledge gaps. *Biosyst. Eng.* **2012**, *114*, 358–371.
7. Marshall, M.; Thenkabail, P. Developing *in situ* Non-Destructive Estimates of Crop Biomass to Address Issues of Scale in Remote Sensing. *Remote Sens.* **2015**, *7*, 808–835.
8. Greenwood, D.J.; Gastal, F.; Lemaire, G.; Draycott, A.; Millard, P.; Neeteson, J.J. Growth rate and %N of field grown crops: Theory and experiments. *Ann. Bot.* **1991**, *67*, 181–190.
9. Lemaire, G.; Jeuffroy, M.-H.; Gastal, F. Diagnosis tool for plant and crop N status in vegetative stage. *Eur. J. Agron.* **2008**, *28*, 614–624.
10. Elia, A.; Conversa, G. Agronomic and physiological responses of a tomato crop to nitrogen input. *Eur. J. Agron.* **2012**, *40*, 64–74.
11. Ntanos, D.A.; Koutroubas, S.D. Dry matter and N accumulation and translocation for Indica and Japonica rice under Mediterranean conditions. *Field Crops Res.* **2002**, *74*, 93–101.
12. Ribbes, F.; Le Toan, T. Rice field mapping and monitoring with RADARSAT data. *Int. J. Remote Sens.* **1999**, *20*, 745–765.
13. Yang, X.; Huang, J.; Wu, Y.; Wang, J.; Wang, P.; Wang, X.; Huete, A.R. Estimating biophysical parameters of rice with remote sensing data using support vector machines. *Sci. China. Life Sci.* **2011**, *54*, 272–281.
14. Li, W.; Li, H.; Zhao, L. Estimating Rice Yield by HJ-1A Satellite Images. *Rice Sci.* **2011**, *18*, 142–147.
15. Lopez-Sanchez, J.M.; Ballester-Berman, J.D.; Hajnsek, I. First Results of Rice Monitoring Practices in Spain by Means of Time Series of TerraSAR-X Dual-Pol Images. *IEEE J. Sel. Top. Appl. Earth Obs. Remote Sens.* **2011**, *4*, 412–422.
16. Koppe, W.; Gnyp, M.L.; Hütt, C.; Yao, Y.; Miao, Y.; Chen, X.; Bareth, G. Rice monitoring with multi-temporal and dual-polarimetric TerraSAR-X data. *Int. J. Appl. Earth Obs. Geoinf.* **2012**, *21*, 568–576.
17. Reddersen, B.; Fricke, T.; Wachendorf, M. A multi-sensor approach for predicting biomass of extensively managed grassland. *Comput. Electron. Agric.* **2014**, *109*, 247–260.
18. Casanova, D.; Epema, G.F.; Goudriaan, J. Monitoring rice reflectance at field level for estimating biomass and LAI. *Field Crops Res.* **1998**, *55*, 83–92.

19. Gnyp, M.L.; Yu, K.; Aasen, H.; Yao, Y.; Huang, S.; Miao, Y.; Bareth, G. Analysis of crop reflectance for estimating biomass in rice canopies at different phenological stages. *Photogramm. Fernerkund. Geoinf.* **2013**, *4*, 351–365.
20. Aasen, H.; Gnyp, M.L.; Miao, Y.; Bareth, G. Automated hyperspectral vegetation index retrieval from multiple correlation matrices with HyperCor. *Photogramm. Eng. Remote Sens.* **2014**, *80*, 785–796.
21. Confalonieri, R.; Bregaglio, S.; Rosenmund, A.S.; Acutis, M.; Savin, I. A model for simulating the height of rice plants. *Eur. J. Agron.* **2011**, *34*, 20–25.
22. Watanabe, T.; Hanan, J.S.; Room, P.M.; Hasegawa, T.; Nakagawa, H.; Takahashi, W. Rice morphogenesis and plant architecture: Measurement, specification and the reconstruction of structural development by 3D architectural modelling. *Ann. Bot.* **2005**, *95*, 1131–1143.
23. Ding, W.; Zhang, Y.; Zhang, Q.; Zhu, D.; Chen, Q. Realistic Simulation of Rice Plant. *Rice Sci.* **2011**, *18*, 224–230.
24. Lee, W.S.; Alchanatis, V.; Yang, C.; Hirafuji, M.; Moshou, D.; Li, C. Sensing technologies for precision specialty crop production. *Comput. Electron. Agric.* **2010**, *74*, 2–33.
25. Zhang, L.; Grift, T.E. A LIDAR-based crop height measurement system for *Miscanthus giganteus*. *Comput. Electron. Agric.* **2012**, *85*, 70–76.
26. Koenig, K.; Höfle, B.; Hämmerle, M.; Jarmer, T.; Siegmann, B.; Lilienthal, H. Comparative classification analysis of post-harvest growth detection from terrestrial LiDAR point clouds in precision agriculture. *ISPRS J. Photogramm. Remote Sens.* **2015**, *104*, 112–125.
27. Gebbers, R.; Ehlert, D.; Adamek, R. Rapid mapping of the leaf area index in agricultural crops. *Agron. J.* **2011**, *103*, 1532–1541.
28. Hosoi, F.; Omasa, K. Estimating vertical plant area density profile and growth parameters of a wheat canopy at different growth stages using three-dimensional portable lidar imaging. *ISPRS J. Photogramm. Remote Sens.* **2009**, *64*, 151–158.
29. Saeys, W.; Lenaerts, B.; Craessaerts, G.; De Baerdemaeker, J. Estimation of the crop density of small grains using LiDAR sensors. *Biosyst. Eng.* **2009**, *102*, 22–30.
30. Eitel, J.U.H.; Vierling, L.A.; Long, D.S.; Raymond Hunt, E. Early season remote sensing of wheat nitrogen status using a green scanning laser. *Agric. For. Meteorol.* **2011**, *151*, 1338–1345.
31. Höfle, B. Radiometric correction of terrestrial LiDAR point cloud data for individual maize plant detection. *Geosci. Remote Sens. Lett. IEEE* **2014**, *11*, 94–98.
32. Hoffmeister, D.; Tilly, N.; Bendig, J.; Curdt, C.; Bareth, G. Detektion von Wachstumsvariabilität in vier Zuckerrübensorten durch multi-temporales terrestrisches Laserscanning. In Proceedings of the 32. GIL-Jahrestagung: Informationstechnologie für eine Nachhaltige Landbewirtschaftung, Freising, Germany, 29 February–1 March 2012; Clasen, M., Fröhlich, G., Bernhardt, H., Hildebrand, K., Theuvsen, B., Eds.; Köllen Verlag: Bonn, Germany, 2012; pp. 135–138.
33. Lumme, J.; Karjalainen, M.; Kaartinen, H.; Kukko, A.; Hyyppä, J.; Hyyppä, H.; Jaakkola, A.; Kleemola, J. Terrestrial laser scanning of agricultural crops. In Proceedings of the International Archives of the Photogrammetry, Remote Sensing and Spatial Information Sciences 37 (Part B5), Beijing, China, 3–11 July 2008; Chen, J.; Jiang, J.; Maas, H.-G., Eds.; Organising Committee of the XXIst International Congress for Photogrammetry and Remote Sensing: Beijing, China, 2008; pp. 563–566.

34. Ehlert, D.; Horn, H.-J.; Adamek, R. Measuring crop biomass density by laser triangulation. *Comput. Electron. Agric.* **2008**, *61*, 117–125.
35. Ehlert, D.; Adamek, R.; Horn, H.-J. Laser rangefinder-based measuring of crop biomass under field conditions. *Precis. Agric.* **2009**, *10*, 395–408.
36. Hämmerle, M.; Höfle, B. Effects of Reduced Terrestrial LiDAR Point Density on High-Resolution Grain Crop Surface Models in Precision Agriculture. *Sensors* **2014**, *14*, 24212–24230.
37. Hosoi, F.; Omasa, K. Estimation of vertical plant area density profiles in a rice canopy at different growth stages by high-resolution portable scanning LiDAR with a lightweight mirror. *ISPRS J. Photogramm. Remote Sens.* **2012**, *74*, 11–19.
38. Tilly, N.; Hoffmeister, D.; Cao, Q.; Lenz-Wiedemann, V.; Miao, Y.; Bareth, G. Precise plant height monitoring and biomass estimation with Terrestrial Laser Scanning in paddy rice. In Proceedings of the ISPRS Annals of the Photogrammetry, Remote Sensing and Spatial Information Sciences Conference, Antalya, Turkey, 11–13 November 2013; Scaioni, M., Lindenbergh, R.C., Oude Elberink, S., Schneider, D., Pirotti, F., Eds.; Volume II-5/W2, pp. 295–300.
39. Tilly, N.; Hoffmeister, D.; Cao, Q.; Huang, S.; Lenz-Wiedemann, V.; Miao, Y.; Bareth, G. Multitemporal crop surface models: Accurate plant height measurement and biomass estimation with terrestrial laser scanning in paddy rice. *J. Appl. Remote Sens.* **2014**, *8*, 083671.
40. Thenkabail, P.S.; Smith, R.B.; De Pauw, E. Hyperspectral vegetation indices and their relationships with agricultural crop characteristics. *Remote Sens. Environ*. **2000**, *71*, 158–182.
41. Hansen, P.M.; Schjoerring, J.K. Reflectance measurement of canopy biomass and nitrogen status in wheat crops using normalized difference vegetation indices and partial least squares regression. *Remote Sens. Environ.* **2003**, *86*, 542–553.
42. Gao, J.; Liu, Y. Climate warming and land use change in Heilongjiang Province, Northeast China. *Appl. Geogr.* **2011**, *31*, 476–482.
43. Domrös, M.; Gongbing, P. *The Climate of China*; Springer-Verlag: Berlin, Germany, 1988.
44. Ding, Y.; Chan, J.C.L. The East Asian summer monsoon: An overview. *Meteorol. Atmos. Phys.* **2005**, *89*, 117–142.
45. Cao, Q.; Miao, Y.; Wang, H.; Huang, S.; Cheng, S.; Khosla, R.; Jiang, R. Non-destructive estimation of rice plant nitrogen status with Crop Circle multispectral active canopy sensor. *Filed Crops Res.* **2013**, *154*, 133–144.
46. Meier, U. *Growth Stages of Mono- and Dicotyledonous Plants*, 2nd ed.; Blackwell: Berlin, Germany, 2001.
47. Lancashire, P.D.; Bleiholder, H.; van den Boom, T.; Langelüddeke, P.; Strauss, R.; Weber, E.; Witzenberger, A. A uniform decimal code for growth stages of crops and weeds. *Ann. Appl. Biol.* **1991**, *119*, 561–601.
48. Riegl LMS GmbH Datasheet Riegl LMS-Z420i. Available online: http://www.riegl.com/uploads/tx_pxpriegldownloads/10_DataSheet_Z420i_03-05-2010.pdf (accessed on 1 July 2014).
49. Riegl LMS GmbH Datasheet Riegl VZ-1000. Available online: http://www.riegl.com/uploads/tx_pxpriegldownloads/DataSheet_VZ-1000_18-09-2013.pdf (accessed on 1 July 2014).

50. Hoffmeister, D.; Bolten, A.; Curdt, C.; Waldhoff, G.; Bareth, G. High resolution Crop Surface Models (CSM) and Crop Volume Models (CVM) on field level by terrestrial laser scanning. In Proceedings of the SPIE, 6th International Symposium on Digital Earth, Beijing, China, 4 November 2010; Guo, H., Wang, C., Eds.; Volume 7840.
51. Besl, P.J.; McKay, N.D. A Method for Registration of 3D Shapes. *IEEE Trans. Pattern Anal. Mach. Intell.* **1992**, *14*, 239–256.
52. Johnston, K.; Ver Hoef, J.M.; Krivoruchko, K.; Lucas, N. *Using ArcGIS Geostatistical Analyst*; ESRI: Redlands, CA, USA, 2001.
53. Willmott, C.J.; Wicks, D.E. An empirical method for the spatial interpolation of monthly precipitation within California. *Phys. Geogr.* **1980**, *1*, 59–73.
54. Willmott, C.J. On the validation of models. *Phys. Geogr.* **1981**, *2*, 184–194.
55. Hair, J.F.; Black, W.C.; Babin, B.J.; Anderson, R.E. *Multivariate Data Analysis*, 7th ed.; Pearson: Upper Saddle River, NJ, USA, 2010.
56. Guarnieri, A.; Pirotti, F.; Vettore, A. Comparison of discrete return and waveform terrestrial laser scanning for dense vegetation filtering. In Proceedings of the International Archives of Photogrammetry, Remote Sensing and Spatial Information Sciences, Melbourne, Australia, 25 August–1 September 2012; Shortis, M., Mills, J., Eds.; Volume 39, pp. 511–516.
57. Velodyne Velodyne HDL-64E User's Manual. Available online: http://www.velodynelidar.com/lidar/products/manual/63-HDL64E S2 Manual_Rev D_2011_web.pdf (accessed on 1 July 2014).
58. Jaakkola, A.; Hyyppä, J.; Kukko, A.; Yu, X.; Kaartinen, H.; Lehtomäki, M.; Lin, Y. A low-cost multi-sensoral mobile mapping system and its feasibility for tree measurements. *ISPRS J. Photogramm. Remote Sens.* **2010**, *65*, 514–522.
59. Ehlert, D.; Heisig, M. Sources of angle-dependent errors in terrestrial laser scanner-based crop stand measurement. *Comput. Electron. Agric.* **2013**, *93*, 10–16.
60. Kaasalainen, S.; Jaakkola, A.; Kaasalainen, M.; Krooks, A.; Kukko, A. Analysis of incidence angle and distance effects on terrestrial laser scanner intensity: Search for correction methods. *Remote Sens.* **2011**, *3*, 2207–2221.
61. Kaasalainen, S.; Krooks, A.; Kukko, A.; Kaartinen, H. Radiometric calibration of terrestrial laser scanners with external reference targets. *Remote Sens.* **2009**, *1*, 144–158.
62. Wang, K.; Zhou, H.; Wang, B.; Jian, Z.; Wang, F.; Huang, J.; Nie, L.; Cui, K.; Peng, S. Quantification of border effect on grain yield measurement of hybrid rice. *Field Crops Res.* **2013**, *141*, 47–54.
63. DigitalGlobe Datasheet WorldView-3. Available online: https://www.digitalglobe.com/sites/default/files/DG_WorldView3_DS_forWeb_0.pdf (accessed on 26 June 2015).
64. Bendig, J.; Yu, K.; Aasen, H.; Bolten, A.; Bennertz, S.; Broscheit, J.; Gnyp, M.L.; Bareth, G. Combining UAV-based plant height from crop surface models, visible, and near infrared vegetation indices for biomass monitoring in barley. *Int. J. Appl. Earth Obs. Geoinf.* **2015**, *39*, 79–87.
65. Wallace, L.; Watson, C.; Lucieer, A. Detecting pruning of individual stems using airborne laser scanning data captured from an Unmanned Aerial Vehicle. *Int. J. Appl. Earth Obs. Geoinf.* **2014**, *30*, 76–85.

66. Luscombe, D.J.; Anderson, K.; Gatis, N.; Wetherelt, A.; Grand-Clement, E.; Brazier, R.E. What does airborne LiDAR really measure in upland ecosystems? *Ecohydrology* **2014**, doi:10.1002/eco.1527.
67. Yao, Y.; Miao, Y.; Huang, S.; Gao, L.; Ma, X.; Zhao, G.; Jiang, R.; Chen, X.; Zhang, F.; Yu, K.; *et al*. Active canopy sensor-based precision N management strategy for rice. *Agron. Sustain. Dev.* **2012**, *32*, 925–933.